DTIC FILE COPY

REPORT SSD-TR-90-24

AD-A227 807

Low-Frequency Ionization-Driven Instability of an Auroral Arc Model

J. M. CORNWALL
Space Sciences Laboratory
Laboratory Operations
The Aerospace Corporation
El Segundo, CA 90245-4691

6 August 1990

Prepared for

SPACE SYSTEMS DIVISION
AIR FORCE SYSTEMS COMMAND
Los Angeles Air Force Base
P.O. Box 92960
Los Angeles, CA 90009-2960

DTIC
ELECTE
OCT 17 1990
S E D

APPROVED FOR PUBLIC RELEASE;
DISTRIBUTION UNLIMITED

This report was submitted by The Aerospace Corporation, El Segundo, CA 90245, under Contract No. F04701-88-C-0089 with the Space Systems Division, Box 92960, Los Angeles, CA 90009-2960. It was reviewed and approved for The Aerospace Corporation by H. R. Rugge, Director, Space Sciences Laboratory.

Lt T. Fisher was the project officer for the Mission-Oriented Investigation and Experimentation (MOIE) Program.

This report has been reviewed by the Public Affairs Office (PAS) and is releasable to the National Technical Information Service (NTIS). At NTIS, it will be available to the general public, including foreign nationals.

This technical report has been reviewed and is approved for publication. Publication of this report does not constitute Air Force approval of the report's findings or conclusions. It is published only for the exchange and stimulation of ideas.

TYRON FISHER, LT, USAF
MOIE Project Officer
SSD/CLPO

JONATHAN EMMES, MAJ, USAF
MOIE Program Manager
AFSTC/WCO OL-AB

UNCLASSIFIED
SECURITY CLASSIFICATION OF THIS PAGE

REPORT DOCUMENTATION PAGE

1a. REPORT SECURITY CLASSIFICATION Unclassified	1b. RESTRICTIVE MARKINGS
2a. SECURITY CLASSIFICATION AUTHORITY 2b. DECLASSIFICATION/DOWNGRADING SCHEDULE	3. DISTRIBUTION/AVAILABILITY OF REPORT Approved for public release; distribution unlimited
4. PERFORMING ORGANIZATION REPORT NUMBER(S) TR-0090(5940-06)-4	5. MONITORING ORGANIZATION REPORT NUMBER(S) SSD-TR-90-24
6a. NAME OF PERFORMING ORGANIZATION The Aerospace Corporation Laboratory Operations 6b. OFFICE SYMBOL *(If applicable)*	7a. NAME OF MONITORING ORGANIZATION Space Systems Division
6c. ADDRESS *(City, State, and ZIP Code)* El Segundo, CA 90245-4691	7b. ADDRESS *(City, State, and ZIP Code)* Los Angeles Air Force Base Los Angeles, CA 90009-2960
8a. NAME OF FUNDING/SPONSORING ORGANIZATION 8b. OFFICE SYMBOL *(If applicable)*	9. PROCUREMENT INSTRUMENT IDENTIFICATION NUMBER F04701-88-C-0089
8c. ADDRESS *(City, State, and ZIP Code)*	10. SOURCE OF FUNDING NUMBERS PROGRAM ELEMENT NO. / PROJECT NO. / TASK NO. / WORK UNIT ACCESSION NO.

11. TITLE *(Include Security Classification)*

Low-Frequency Ionization-Driven Instability of an Auroral Arc Model

12. PERSONAL AUTHOR(S)

Cornwall, John M.

13a. TYPE OF REPORT	13b. TIME COVERED FROM _____ TO _____	14. DATE OF REPORT *(Year, Month, Day)*	15. PAGE COUNT
		1990 August 6	33

16. SUPPLEMENTARY NOTATION

17. COSATI CODES			18. SUBJECT TERMS *(Continue on reverse if necessary and identify by block number)*
FIELD	GROUP	SUB-GROUP	Auroral ionosphere

19. ABSTRACT *(Continue on reverse if necessary and identify by block number)*

The low-frequency (time scales of tens of seconds) dynamics of the auroral ionosphere differs from that of the nonauroral ionosphere by the presence of strong, unstable space-and-time-dependent ionospheric ionization produced by precipitating auroral electrons. If recombination is relatively unimportant (as at high ionospheric heights), we show that in general transport processes cannot remove this ionization as fast as it is created, and no equilibrium is possible. We investigate these nonequilibrium phenomena in the context of a nonlinear adiabatic auroral model, which has previously been studied in static situations. We give a linearized local perturbation analysis of what amounts to a current-driven E X B gradient-drift instability with an ionization source, as well as some exact nonlinear solutions valid in a finite but limited spatial region. These solutions show continuing motion of auroral potential and plasma density as the aurora tries to shift its ionization problems from one place to another. The analysis gives clues to the possibility of generation of chaos and of fine-scale spatial structure.

20. DISTRIBUTION/AVAILABILITY OF ABSTRACT ☒ UNCLASSIFIED/UNLIMITED ☐ SAME AS RPT. ☐ DTIC USERS	21. ABSTRACT SECURITY CLASSIFICATION Unclassified
22a. NAME OF RESPONSIBLE INDIVIDUAL	22b. TELEPHONE *(Include Area Code)* / 22c. OFFICE SYMBOL

DD FORM 1473, 84 MAR — 83 APR edition may be used until exhausted. All other editions are obsolete

SECURITY CLASSIFICATION OF THIS PAGE
UNCLASSIFIED

PREFACE

This work was supported in part by NASA Grant NAGW 1613.

Accession For
NTIS CRA&I
DTIC TAB
Unannounced
Justification
By
Distribution/
Availability Codes
Avail and/or
Dist Special
A-1

CONTENTS

1. INTRODUCTION 5

2. PRELIMINARIES 11

3. ABSENCE OF GENERIC EQUILIBRIUM AT $\alpha = 0$ 15

4. LOCAL PERTURBATION THEORY 17

5. INTEGRABLE MODEL OF TRANSPORT-IONIZATION COMPETITION 21

6. DISCUSSION 31

REFERENCES 33

APPENDIX A-1

FIGURES

1. Potentials and Density at $y = 0$ for a Steady-State Solution with Recombination 22

2. Potentials and Density at $\tau = 0$, $y = 0$ for a Time-Dependent Solution with no Recombination 28

3. Potentials and Density at $\tau = 2$, $y = 0$ for a Time-Dependent Solution with no Recombination 29

1. INTRODUCTION

The adiabatic auroral arc model [Chiu and Schulz, 1978; Chiu and Cornwall, 1980; Chiu et al., 1981; Lyons, 1980, 1981] is a reasonable if incomplete description of a time-independent auroral arc driven by a large-scale parallel potential drop (as seen experimentally; see, e.g., Reiff et al. [1988]). Even the static properties of the model are difficult to investigate because the defining equations are nonlinear, but recently Cornwall [1988] has found some exact two-dimensional (latitude and longitude; height dependence suppressed by height integration) stationary solutions.

The next step in investigating the model is to look at the low-frequency dynamics, which is expected to show unstable Kelvin-Helmholtz [e.g., Hallinan and Davis, 1970] modes and possibly other interchange modes as well. Several physically different time scales are contained in the adiabatic model, and they all turn out to be in the range of tens of seconds:

Ionization growth time $$T_I = \frac{eN}{\Gamma Q \Delta\phi} \simeq 30 \text{ sec} \tag{1.1}$$

$\underset{\sim}{E} \times \underset{\sim}{B}$ drift transport time $$T_P = \frac{B\Lambda^2}{c\Delta\phi} \simeq 50 \text{ sec} \tag{1.2}$$

Dissociative recombination time $$T_R = (2\alpha N)^{-1} \simeq 50 \text{ sec} \tag{1.3}$$

In these equations, c, e, and B are the speed of light, the electronic charge, and the Earth's magnetic field, respectively, and the other quantities and their nominal values are:

Height-integrated ionospheric plasma density $N \simeq 10^{12}$ cm^{-2}

Number of ion pairs per incident auroral primary $\Gamma \simeq 30$

Current-potential parameter Q $\simeq 0.1\text{-}0.2$ cm^{-1} sec^{-1} (see (1.4) below)

Nominal parallel potential drop $\Delta\phi$ $\Delta\phi \simeq 1.5$ kV

Height-integrated dissociative recombination rate α $\simeq 10^{14}$ cm^{-2} sec^{-1}

Inverted-V scale length Λ $\approx$ 40 km (see (2.7) below)

Many of these parameters can deviate substantially from their nominal values, especially as the parallel potential drop changes, and so one or another of the three time scales in (1.1,2,3) may dominate (i.e., be smallest). For example, a low-energy aurora may not penetrate to the heights where dissociative recombination is important, so α will be much smaller then nominal. Or just after an aurora turns on in the midnight ionosphere, N may be an order of magnitude smaller than nominal, and again recombination is unimportant. In writing the nominal parameter values we have not attempted to construct an internally consistent set; later in applications we will be more precise.

There are, of course, a host of other time and space scales that one might invoke in auroral dynamics associated with local wave modes: (drift, ion cyclotron, lower hybrid, ...) or with magnetospheric phenomena (wave, particle quarter-bounce times, polarization currents, Pc 1-5 waves, reconnection time scales). Also there are correspondingly many studies of phenomena associated with these scales, as well as the ones that concern us; for example, Basu et al. [1988], Gorney [1989], Weimer et al. [1985, 1987] study the spatial scales of auroras from 0.1 to 100 km in the ionosphere or magnetosphere. Theories to explain the resulting power spectra are reviewed in Kintner and Seyler [1985]; Keskinen and Ossakow [1983]; Fejer [1989]; and Huba [1989]. In most cases theoretical analysis does not go beyond linear instabilities, and is then supplemented with large computer simulations, such as that of Mitchell et al. [1985] for high-latitude F-layer instabilities and of Keskinen et al. [1988] for Kelvin-Helmholtz (KH) instability in the high-latitude ionosphere. Linear analysis is complicated by the need to account for the destabilizing effects of auroral gradients, whether on large scales for such modes as Kelvin-Helmholtz, or on small scales (e.g., Ganguli et al. [1985]; Basu and Coppi [1989]). The particular mechanisms we emphasize, namely a parallel current driven by a parallel potential drop and the consequent ionization of the auroral ionosphere, also have consequences on spatial scales larger than the typical transverse width of an inverted-V, such as current oscillations on scales of hundreds of km [Weimer et al., 1988] and modification of large-scale convection fields (e.g., Blomberg and Marklund [1988]). Finally, these mechanisms can react on the driving magnetospheric source, causing feedback

effects which we do not attempt to analyze here [Lotko et al., 1987].

On the one hand we would like to incorporate all these effects into a comprehensive model of time-dependent auroral dynamics, but so far that is out of the question. On the other hand, there is as yet little theoretical work and no simulations which include the specific effects mentioned above which are the hallmarks of the adiabatic auroral model. The first is an auroral parallel current $J_{\parallel}$ (positive upward) whose strength is linear in the difference in potential between the ionosphere (ϕ) and the equator (ϕ_E):

$$J_{\parallel} = Q(\phi-\phi_E) \ . \tag{1.4}$$

The second is an auroral ionization source, of strength $\Gamma J_{\parallel}/e$, where Γ is the number of electron-ion pairs produced by a single auroral primary. In principle, Γ itself depends linearly on $\phi-\phi_E$ (since Γ is the ratio of the auroral primary energy to the energy needed to form a pair), but for the most part in this report we will take Γ to be a given constant; this does not affect any of our qualitative conclusions (cf. Cornwall [1988] who studied both cases for Γ for the static auroral arc model). The ionization sources we use in this report, and their significant effects on auroral-ionospheric densities that we find, are consistent with experimental studies of spatially structural auroral ionization produced by precipitating electrons [Labelle et al., 1989].

The purpose of the present report is to study, in an analytical way, the influence of the ionization source represented by $J_{\parallel}$ when recombination is insufficient to bring about equilibrium; that is, when T_R of (1.3) is long compared to T_I of (1.1). This can happen, in particular, for low-energy auroras which deposit their energy at altitudes where dissociative recombination is small. One might then expect that transport processes would take over, yielding an equilibrium where ionization is transported to the return-current region as fast as it is produced in the aurora. But we show that this is generally impossible; there are always regions where horizontal transport vanishes or is very small. There are then at least three possibilities to control the growth of ionization in such a region: (1) the region of small horizontal transport moves elsewhere; (2) vertical downward transport to altitudes where recombination is effective takes place; (3) the ionospheric potential ϕ decreases, thus lowering the ionization source strength (see (1.4)).

In this report, we concentrate on possibilities (1) and (3) above, and we will find that they indeed are important. As for possibility (2), vertical transport, the projection of neutral winds along $\underset{\sim}{B}$ in the auroral zone is too small to be important, and the vertical component of such winds in the aurora is upward (because of auroral heating). Upward winds act in the wrong direction to bring excess ionization downward, but they can raise molecular ions to greater altitudes, thus promoting dissociative recombination there. But the upward velocity is only a few m/sec, too small to matter. It is true that the upward vertical winds are deflected into horizontal flow which would carry ionization out of the aurora, in a horizontal flow pattern which appears to have a strong divergence, but the wind speeds in these cells is only tens of m/sec, too small to be important.

We will analyze the problem of ionization-driven auroral dynamics in two ways. The first is traditional local perturbation theory, which yields a long-wavelength growth rate with a term proportional to the ionization rate Γ. Other terms enter at shorter wavelengths which we identify with corresponding terms in the usual $\underset{\sim}{E} \times \underset{\sim}{B}$ -gradient-drift instability; one expects that in general these transport terms tend to damp the instability, but this need not always be the case. Finally, there are terms which represent the direct influence of the parallel current $J_{\parallel}$ of (1.4). Their effect is not comparable to parallel currents in the current-driven $\underset{\sim}{E} \times \underset{\sim}{B}$ -gradient-drift instability, where a parallel current perturbation involves a density perturbation. Evidently from (1.4) a perturbation in $J_{\parallel}$ is a perturbation in ϕ, which has quite different consequences. It is more appropriate to describe our instability as an ionization-driven $\underset{\sim}{E} \times \underset{\sim}{B}$ -gradient-drift instability.

Second, we are able to find some locally exact solutions to the full nonlinear equations of the model. We call them "locally exact" because while they are indeed exact solutions, the assumed spatial dependence (namely, quadratic) of the height-integrated density N and the potential ϕ is not sufficiently general to admit extension to the entire auroral region out to the return-current boundary. (There are one or two relatively uninteresting globally exact time-dependent solutions, which we mention in Section 5.) These locally exact solutions show the phenomena mentioned above, in which the regions of small transport move and the ionospheric potential ϕ decreases. As time passes, these phenomena will begin to happen somewhere else in the aurora, which thus shows a ceaseless pattern of movement. It will be

interesting to study (as we intend to at a later date) the dynamics with a computer, to go beyond the locally exact results.

What we have found so far gives several hints as to what might happen beyond this locally exact description. First, a slight generalization of the hypothesized spatial dependence for N and ϕ yields four coupled nonlinear ordinary differential equations in time which are not obviously integrable; if they are in fact not integrable, their solution (and *a fortiori* more general solutions with no restrictions on spatial dependence) will be chaotic. Second, linear perturbation theory couples the ionization source to the $\underset{\sim}{E} \times \underset{\sim}{B}$ -gradient-drift instability, and the latter, by itself, leads to development of spatial structure at finer and finer scales, through a process of bifurcation. This might happen in the full nonlinear model as well.

Finally, a comment on the role of recombination, which we assume is small for purposes of this report. Because dissociative recombination depends on N^2, given enough time it can equilibrate any ionization source which grows less rapidly with N. However, this cuts the other way too: in the midnight auroral ionosphere during the absence of auroral activity, N is small enough so that dissociative recombination is really quite small, and the time scale is much larger than given in (1.3). When we speak of absence of equilibrium, we mean that the time between auroral turn-on and recombination dominance is rather long compared to the ionization time scale in (1.1).

The report is organized as follows: Section 2 sets the stage and introduces the model equations. Section 3 gives the proof that there are always regions where transport cannot balance ionization. Section 4 gives the local perturbative analysis, and Section 5 gives the locally exact solutions. An Appendix gives a slight generalization of Section 5's equations which may have chaotic solutions.

2. PRELIMINARIES

The essence of the model is to leave out all phenomena taking place on time scales much less than tens of seconds. For certain effects this can be justified, while for others it may be an idealization.

Auroral electron (and even auroral proton) quarter-bounce times are smaller than tens of seconds, so we will not account for delay times in propagating particles from the source region to the ionosphere. (This is not true for Alfvén-wave bounce times, or wave periods, which are quite comparable to our auroral time scales; it would be interesting to study the coupling of the auroral ionosphere to ULF waves in a model similar to ours.) We can in effect ignore polarization currents, whose effects compared to Pedersen currents are in the ratio [Mitchell et al., 1985; Cornwall, 1988]

$$\frac{\omega C_M}{\Sigma_P} \simeq 0.1\text{-}0.2 \tag{2.1}$$

where $\omega \simeq 0.1\ \mathrm{sec}^{-1}$ is a typical frequency, Σ_P is the height-integrated Pedersen conductivity ($\simeq$5-10 mho in an aurora) and $C_M \simeq 10$ farad is the height-integrated magnetospheric capacitance:

$$C_M = B_I \int \frac{dz}{B} \frac{c^2}{4\pi V_A{}^2} \tag{2.2}$$

(here V_A is the Alfvén velocity and B_I the ionospheric magnetic field). Moreover, at these low frequencies the magnetosphere acts as an integrated unit since wave and particle quarter-bounce frequencies are at least as large as those that interest us. (Mitchell et al. [1985] and Keskinen et al. [1988] have studied a case opoosite to ours, where no currents of the type (1.4) are kept, but polarization currents are retained.) Similarly we treat the ionosphere as a unit in altitude by height-integrating.

Which height region of the ionosphere we should integrate over depends on the energy of the auroral primaries, which determines their penetration depth. We will usually require

$$\omega \ll \nu \ll \Omega \tag{2.3}$$

where ν is the ion-neutral collision frequency, and Ω the ion (we assume O^+)

gyrofrequency. The first inequality allows us to ignore polarization currents, while the second allows us to drop Hall currents and to approximate the ion drift velocity by that due to $\underset{\sim}{E} \times \underset{\sim}{B}$ drift. Inequality (2.3) implies that the aurora does not penetrate below ≈150 km (corresponding to primary energies of only a keV or so); for example, at 200 km $\nu_{iN} \simeq 3\ sec^{-1}$, $\Omega \simeq 200\ sec^{-1}$. As for height integration of the recombination rate, this depends not only on the dissociative-recombination coefficient α but also on the atomic ion-molecule interchange rate at higher altitudes, which form the necessary molecular ions from the preponderant O^+ ions. Rather than introduce the extra complication of ion-molecule interchange, we will consider only two cases: predominance of molecular ions and square-law recombination, or linear and relatively unimportant recombination at higher altitudes.

With these assumptions, plus quasineutrality, the equations to be solved are [Cornwall, 1988]:

$$\underset{\sim}{\nabla} \cdot (\Sigma_P \underset{\sim}{\nabla} \phi) = Q(\phi - \phi_E) \tag{2.4}$$

$$\frac{\partial N}{\partial t} + \underset{\sim}{V}_E \cdot \underset{\sim}{\nabla} N = \frac{\Gamma Q}{e} (\phi - \phi_E) - \alpha(N^2 - N_o^{\ 2}) \ . \tag{2.5}$$

In these equations all vectors are two-dimensional, and we take the x coordinate to point north and the y coordinate to point east; $\underset{\sim}{B}$ is constant and points vertically downward. The term $-\alpha(N^2-N_o^{\ 2})$ in the continuity equation (1.9) includes not only square-law dissociative recombination but also any non-auroral ionization sources ($\alpha N_o^{\ 2}$). In certain circumstances we omit the term $-\alpha(N^2-N_o^{\ 2})$ from (2.5). In (2.5), the electric drift velocity is

$$\underset{\sim}{V}_E = \frac{c}{B} (\underset{\sim}{E} \times \hat{b}) = \frac{c}{B} (-\partial_y \phi, \partial_x \phi) \ ; \tag{2.6}$$

it is divergence-free. As is well-known, the current-conservation equation (2.4) defines a fundamental scale length Λ:

$$\Lambda^2 = \Sigma_P / Q \tag{2.7}$$

with Λ of the order of several tens of km. Later we will see that V_E-driven transport leads to a new scale length Λ_T, given by

$$\Lambda_T = \Lambda\left(\frac{Nce}{\Gamma B \Sigma_P} \right)^{1/2} \tag{2.8}$$

which is nominally about $(1/2)\Lambda$. This is the gradient scale length where transport processes begin to compete with ionization.

3. ABSENCE OF GENERIC EQUILIBRIUM AT $\alpha = 0$

In Cornwall [1988] it was shown that Eqs. (2.4,5) do have equilibrium solutions of a special type, in which there is a functional relation between N and ϕ (and, of course, ϕ_E is stationary). Given such a relation, the $\underset{\sim}{E} \times \underset{\sim}{B}$ current $N\underset{\sim}{V}_E$ is identically conserved, and disappears from (2.5). These equilibria can be two-dimensional and depend on a balance between ionization sources (first term on the RHS of (2.5)) and recombination losses. Presumably other equilibrium solutions exist in which N is not functionally related to ϕ, but they are not known analytically; in that case, transport would also play a role in balancing sources and losses.

The situation is different when recombination is unimportant. We show that **Eqs. (2.4,5) with $\alpha = 0$ generically have no time-independent solutions for an aurora**. The reason is that there must be places where $\underset{\sim}{V}_E \cdot \underset{\sim}{\nabla} N$ vanishes, so there is nothing left to balance the ionization created by auroral primaries.

An aurora generally has return-current boundaries: two lines, running more or less east-west, along which $\phi = \phi_E$. Inside this strip--the aurora itself--we have $\phi - \phi_E > 0$. Outside the strip defined by these lines, the ionospheric density N returns to an ambient value N_o, but it is bigger than N_o inside. It follows that for every fixed y, N has at least one maximum in x, where $\partial_x N = 0$. This equation, $\partial_x N(x,y) = 0$, defines a line in the aurora also going more or less east-west. As we follow this line (say, by increasing y) we must encounter at least one value of y where $\partial_y N = 0$ also, since otherwise N would continually increase or decrease as we go. So there is at least one point where $\underset{\sim}{V}_E \cdot \underset{\sim}{\nabla} = 0$ (because $\underset{\sim}{\nabla} N = 0$), and by continuity a finite region including this point where transport cannot balance auroral ionization.

We can similarly show that $\underset{\sim}{V}_E$ has zeroes or near-zeroes. For a generic aurora, V_{Ey} changes sign in going from one return-current boundary to the other at any fixed y; this corresponds to the characteristic change of sign of E_x seen in auroras. The equation $V_{Ey}(x,y) = 0$ again defines a line running more or less east-west, characterized by an infinitesimal tangent vector $d\underset{\sim}{\ell}$. Along this line $E_x = 0$, and since $\underset{\sim}{\nabla} \times \underset{\sim}{E} = 0$, we have

$$\oint d\underset{\sim}{\ell} \cdot \underset{\sim}{E} = 0 \ , \tag{3.1}$$

where the integral goes around the auroral zone. Since $d\underset{\sim}{\ell}$ is more or less in the y-direction, (3.1) implies there is at least one place where $E_y \simeq 0$. Consequently there is one or more places where $\underset{\sim}{V}_E \simeq 0$ and transport is negligible or zero. If recombination is small, again there is nothing to balance the buildup of ionization produced by auroral primaries.

The equation

$$\underset{\sim}{\nabla} \cdot (N\underset{\sim}{V}_E) = 0 \tag{3.2}$$

has, as we have just seen, at least one solution, say at $x = x_o$, $y = y_o$ (which in general are functions of t). This equation is a continuous function of x and y, so its zeroes generically define a line $f(x,y) = 0$ where transport is negligible. In a finite region around each point of this line transport cannot be in equilibrium with ionization production, so in general the auroral region inside the return-current boundaries has strips of finite width where equilibrium is impossible.

Given these strips, what is the qualitative nature of the evolution in time of the basic equations (2.4,5)? We begin to answer that question in the next section with a study of linear perturbations, and then go on to fully nonlinear and exact solutions.

4. LOCAL PERTURBATION THEORY

Local perturbation theory can be at best a heuristic guide, since the essence of auroral dynamics is the steep density gradients related to ionization and transport processes. Nonetheless, we will find here a useful introduction to the exact solutions of the next section.

We linearize Eqs. (2.4,5), writing

$$N = N_o(\underset{\sim}{x}) + N_1 \, e^{i(\underset{\sim}{k}\cdot\underset{\sim}{x}-\omega t)} \tag{4.1}$$

$$\phi = \phi_o(\underset{\sim}{x}) + \phi_1 \, e^{i(\underset{\sim}{k}\cdot\underset{\sim}{x}-\omega t)} \quad . \tag{4.2}$$

The linearized equations are:

$$-i\omega N_1 + i\,\frac{c}{B}\,[k_x\phi_1\,\partial_y N_o - k_y\phi_1\,\partial_x N_o + k_y N_1\,\partial_x\phi_o - k_x N_1\partial_y\phi_o]$$
$$- \frac{\Gamma Q}{e}\,\phi_1 + 2\alpha N_o N_1 = -\frac{\Gamma Q}{e}\,\phi_{E1} \tag{4.3}$$

$$iN_1\,\underset{\sim}{k}\cdot\underset{\sim}{\nabla}\phi_o + i\phi_1\,\underset{\sim}{k}\cdot\underset{\sim}{\nabla}N_o - k^2\phi_1 N_o + N_1\nabla^2\phi_o - \left(\frac{N_o}{\Lambda_o^{\,2}}\right)\phi_1$$
$$= -\left(\frac{N_o}{\Lambda_o^{\,2}}\right)\phi_{E1} \quad . \tag{4.4}$$

The scale length $\Lambda_o^{\,2}$ is defined via (2.7):

$$\Lambda_o^{\,2} = \Sigma_p(N{=}N_o)/Q \quad . \tag{4.5}$$

To find the dispersion relation, we drop the inhomogeneous perturbation ϕ_{E1}. Straightforward algebra gives:

$$\omega - \underset{\sim}{k}\cdot\underset{\sim}{V}_{Eo} = -2i\alpha N_o + \left[\, i\,\frac{\Gamma Q}{e} + \frac{c}{B}\,(k_x\partial_y - k_y\partial_x)\,N_o \,\right]$$
$$\times \frac{(i\underset{\sim}{k}\cdot\underset{\sim}{\nabla}\phi_o + \nabla^2\phi_o)}{[-i\underset{\sim}{k}\cdot\underset{\sim}{\nabla}N_o + N_o(k^2+\Lambda_o^{\,-2})]} \quad . \tag{4.6}$$

Here $\underset{\sim}{V}_{Eo}$ is the electric drift velocity (2.6) at $\phi = \phi_o$.

There are several potential instabilities in this formula. First, for long wavelengths ($k\Lambda_o \ll 1$) one finds

$$\mathrm{Im}\ \omega = \frac{\Gamma Q}{eN_o}\ (\Lambda_o^{\ 2}\nabla^2\phi_o) - 2\alpha N_o\ . \tag{4.7}$$

The first term on the RHS is always positive, and is at least as large as T_I^{-1} as defined in (1.1). These statements follow from the equation (2.4) satisfied by ϕ_o:

$$\nabla^2\phi_o = \frac{(\phi_o - \phi_E)}{\Lambda_o^{\ 2}} - \frac{1}{N_o}\ \underset{\sim}{\nabla}\phi_o \cdot \underset{\sim}{\nabla} N_o\ . \tag{4.8}$$

In an aurora $\phi_o - \phi_E$ is positive, and $\underset{\sim}{\nabla}\phi_o \cdot \underset{\sim}{\nabla} N_o$ is generically negative, so $\Lambda_o^{\ 2}\nabla^2\phi_o$ is positive and greater than the potential drop $\phi_o - \phi_E$.

This ionization-driven instability ultimately will be controlled by recombination, transport, or decrease of the parallel potential drop. Transport phenomena are important at large $\underset{\sim}{k}$, where it can be seen from (4.6) that the ionization term ($-\Gamma$) is small. At large $\underset{\sim}{k}$ ($k\Lambda_o \gg 1$) we find:

$$\mathrm{Im}\ \omega \rightarrow \gamma \equiv N_o^{\ -1}(\underset{\sim}{V}_{Eo} \cdot \underset{\sim}{\nabla} - \hat{k} \cdot \underset{\sim}{V}_{Eo}\hat{k} \cdot \underset{\sim}{\nabla})\ N_o - 2\alpha N_o\ , \tag{4.9}$$

where $\hat{k}$ is the unit vector in the direction of $\underset{\sim}{k}$. The terms in V_{Eo} can be of either sign, a negative contribution representing damping of the ionization-driven instability. A positive term is just a version of the standard $\underset{\sim}{E} \times \underset{\sim}{B}$ gradient-drift instability [e.g., Linson and Workman, 1970]. In any case, the magnitude of this sort of term in Im ω is of the order of the inverse drift-transport time T_D^{-1} (see (1.2)). Simple geometric considerations show that terms of both signs are likely to be present in a fully developed aurora, that is, one with significant E-W gradients.

We can roughly estimate the cross-over scale length Λ_D where drift-transport and ionization contributions to Im ω are comparable, by equating these contributions from (4.6) and solving for $k = \Lambda_D^{-1}$. In so doing, assume the scale lengths of N_o and ϕ_o are the same, and ignore geometrical factors. One then finds

$$\Lambda_D = \left(\frac{cN_o e}{B\Gamma Q}\right)^{1/2} = \Lambda_o\left(\frac{cN_o e}{B\Gamma\ \Sigma_{Po}}\right)^{1/2}\ , \tag{4.10}$$

where in the second equality we used (2.7). For the nominal parameter values given in Section 1, Λ_D is roughly $(1/2)\Lambda_o$, but this depends somewhat on the auroral energy. Low energy auroras have smaller values for both Γ and Σ_{Po}

than high-energy auroras, because they operate at higher altitudes and because they make fewer electron-ion pairs.

It is interesting to consider now the inhomogeneous problem, in which the perturbation ϕ_{E1} in the driving magnetospheric potential is retained. In earlier work [Chiu et al., 1981] it was observed that in the static adiabatic auroral model, small-scale ($k\Lambda \gg 1$) fluctuations in ϕ_E were shielded from the ionosphere, while fluctuations with $k\Lambda \gtrsim 1$ were not shielded. This makes it difficult to understand small-scale auroral ionospheric fluctuations as being straightforwardly driven from the magnetosphere. Weimer et al. [1985] have confirmed this shielding effect experimentally. Making the approximations of a time-stationary aurora and constant Σ_p, they used the simplified relation which then follows from (2.4), or equivalently from (4.4) by setting N_1 and $\nabla N_o = 0$:

$$\phi_1(\underset{\sim}{k}) = \frac{\phi_{E1}(\underset{\sim}{k})}{1+k^2\Lambda_o^2} \tag{4.11}$$

(where ϕ_1 is the Fourier transform of ϕ, etc.) and found it to be reasonably well-satisfied. However, at non-zero frequencies this shielding effect should diminish. The reduction of shielding can be seen even at the low frequencies of interest in the present report, by solving the full inhomogeneous equations (4.3,4). We give the results only for $k\Lambda_o \gg 1$:

$$\phi_1(\underset{\sim}{k},\omega) = \frac{\phi_{E1}(\underset{\sim}{k},\omega)}{k^2\Lambda_o^2}\left\{1 + \frac{1}{\omega-\underset{\sim}{k}\cdot\underset{\sim}{V}_{Eo}-i\gamma}\left[i\gamma + \frac{\Lambda_o^2\Gamma Q}{N_o e}\,\underset{\sim}{k}\cdot\underset{\sim}{\nabla}\phi_o\right]\right\}, \tag{4.12}$$

where γ (defined in (4.9)) is the large-k limit of Im ω. In the approximations used by Weimer et al. [1985], namely $\nabla N_o = 0$, $\Gamma = 0$, one has $\gamma = 0$ and so (4.12) is just the large-k limit of (4.11). But when these approximations are not valid, the terms in square brackets come into play. For example, in an aurora with no E-W variation ($k_y = \partial_y = 0$) we find that (4.12) is, for large k:

$$\phi_1(k,\omega) = \phi_{E1}(k,\omega)\,\frac{V_{Eo}}{(\omega-i\gamma)}\,\frac{1}{k\Lambda_D^2} \tag{4.13}$$

which decreases only like k^{-1}.

5. INTEGRABLE MODEL OF TRANSPORT-IONIZATION COMPETITION

As discussed in the Introduction, when $\alpha = 0$ (no recombination) equilibrium is generally impossible, because there are regions where transport is too small to balance ionization. Here we illustrate what goes on in the vicinity of a zero in the transport term $\underset{\sim}{V}_E \cdot \underset{\sim}{\nabla} N$ in (2.5) when $\alpha = 0$, by postulating that N and ϕ in (2.4,5) are no more than quadratic in spatial variables, with time-dependent coefficients. Remarkably, these nonlinear partial differential equations fall apart into four **integrable** ordinary differential equations in time, whose solutions show the slow wandering of auroral features discussed in the Introduction.

The particular spatial dependence used to get these results is not the most general quadratic dependence. We briefly study the most general quadratic case in the Appendix, and find four nonlinear first-order differential equations in the time variable. These equations are not obviously integrable. If they are in fact not integrable, they may develop chaotically, an interesting possibility which will require computer studies.

Consider now Eqs. (2.4,5) with $\alpha = 0$. We seek a solution of the form

$$\phi = \tilde{\phi} + \tilde{\phi}_1 x + \tilde{\phi}_2 y + \tilde{\phi}_3 x^2 \tag{5.1}$$

$$N = \tilde{N} + \tilde{N}_1 x + \tilde{N}_2 y + \tilde{N}_3 x^2 \tag{5.2}$$

$$\phi_E = \tilde{\phi}_E x^2 \ . \tag{5.3}$$

Here all the functions with tildes depend on time only. Recall that the x-variable runs north-south and y runs east-west. We require that the driving potential $\tilde{\phi}_E$ be positive, and that $\tilde{N}_3$ be negative, so that there is a density peak at $x = 0$ and a horizontal electric field with negative divergences. We also require that $\tilde{\phi} > 0$ so that near the origin (x=y=0) the ionospheric potential exceeds ϕ_E, which has a minimum there. This is a typical configuration for auroral arcs. In a **static** arc (stabilized, e.g., by recombination) one usually looks for ϕ to have a minimum and N a maximum at the same point where ϕ_E has a minimum; an example is Fig. 1 (adapted from Cornwall [1988]). We can arrange this as an initial condition by setting $\tilde{\phi}_1(0) = \tilde{N}_1(0) = 0$ in (5.1,2), but we will see that as time passes, the extrema

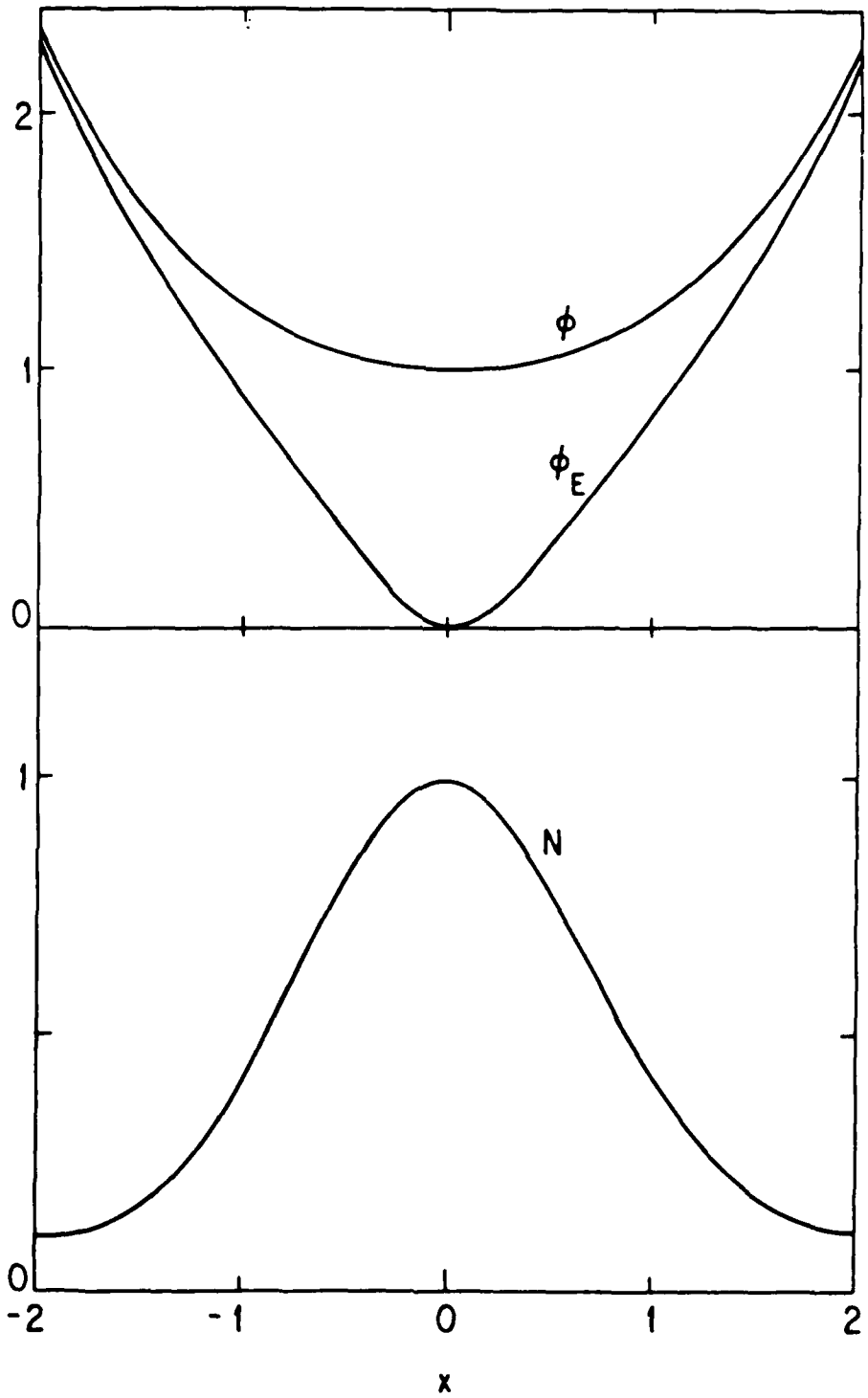

Fig 1. Potentials and Density at y = 0 for a Steady-State Solution with Recombination (after Cornwall [1988]). The return-current region is displaced to $|x| = \infty$, where N returns to its asymptotic value of 0.1 (in units of the density at x = 0) and $\phi = \phi_E$. The distance scale is in units of Λ_o.

of ϕ and N wander away from each other and from the minimum of ϕ_E, thus rearranging the relative strengths of ionization sources and transport.

The ansatz (5.1,2,3) can be generalized by adding terms $-xy$ or y^2; this case is briefly discussed in the Appendix, but we know of no way of integrating this general case.

Using the ansatz in Eq. (2.4) yields four relations. In writing these relations we temporarily drop the tildes on the variables, so that ϕ and N refer to only the spatially constant parts of what we usually mean by these names. These relations are:

$$2\phi_3 N + N_1\phi_1 + N_2\phi_2 = \frac{N_o}{\Lambda_o^2}\,\phi \tag{5.4}$$

$$4\phi_3 N_1 + 2N_3\phi_1 = \frac{N_o}{\Lambda_o^2}\,\phi_1 \tag{5.5}$$

$$2\phi_3 N_2 = \frac{N_o}{\Lambda_o^2}\,\phi_2 \tag{5.6}$$

$$6\phi_3 N_3 = \frac{N_o}{\Lambda_o^2}\,(\phi_3-\phi_E)\ . \tag{5.7}$$

Here we have introduced an arbitrary density N_o and length scale Λ_o, related by

$$\Lambda_o^2 = \Sigma_P(N=N_o)/Q\ . \tag{5.8}$$

Eq. (2.5) similarly yields four differential equations:

$$\dot{N} + \frac{c}{B}\,(N_2\phi_1 - N_1\phi_2) = \frac{\Gamma Q}{e}\,\phi \tag{5.9}$$

$$\dot{N}_1 + \frac{2c}{B}\,(N_2\phi_3 - \phi_2 N_3) = \frac{\Gamma Q}{e}\,\phi_1 \tag{5.10}$$

$$\dot{N}_2 = \frac{\Gamma Q}{e}\,\phi_2 \tag{5.11}$$

$$\dot{N}_3 = \frac{\Gamma Q}{e}\,(\phi_3-\phi_E)\ . \tag{5.12}$$

We can eliminate all the ϕ-variables in terms of the N-variables and ϕ_E, using Eqs. (5.4-7):

$$\phi = \frac{2\Lambda_o^2}{N_o}\phi_E\left(1 - 6\Lambda_o^2\frac{N_3}{N_o}\right)^{-1}\left(N + \frac{\Lambda_o^2 N_2^2}{N_o} + 4N_1^2\left(\frac{N_o}{\Lambda_o^2} - 2N_3\right)^{-1}\right) \tag{5.13}$$

$$\phi_1 = 4N_1\phi_E\left[\left(\frac{N_o}{\Lambda_o^2} - 2N_3\right)\left(1 - 6\Lambda_o^3\frac{N_3}{N_o}\right)\right]^{-1} \tag{5.14}$$

$$\phi_2 = \frac{2\Lambda_o^2 N_2}{N_o}\left(1 - 6\Lambda_o^2\frac{N_3}{N_o}\right)^{-1} \tag{5.15}$$

$$\phi_3 = \phi_E\left(1 - 6\Lambda_o^2\frac{N_3}{N_o}\right)^{-1} \tag{5.16}$$

These equations can be partially non-dimensionalized by agreeing to measure all densities in units of N_o and all lengths in units of Λ_o, in which case the explicit factors of $N_o\Lambda_o^{-2}$ in (5.13-16) should be set to 1; N and the N_i ($i = 1,2,3$) are dimensionless; and ϕ_E is the driving potential at $x = \Lambda_o$. We adopt these scalings in writing the differential equations (5.9-12) in terms of N and the N_i:

$$\dot{N}_3 = \frac{\Gamma Q\phi_E}{eN_o}\left(\frac{6N_3}{1-6N_3}\right) \tag{5.17}$$

$$\dot{N}_2 = \frac{\Gamma Q\phi_E}{eN_o}\frac{2N_2}{1-6N_3} \tag{5.18}$$

$$\dot{N}_1 = \frac{1}{1-6N_3}\left\{\left(\frac{4\Gamma Q\phi_E}{eN_o}\right)\left(\frac{N_1}{1-2N_3}\right) - \left(\frac{2c\phi_E}{B\Lambda_o^2}\right)N_2(1-2N_3)\right\} \tag{5.19}$$

$$\dot{N} = -\frac{2c\phi_E}{B\Lambda_o^2}\frac{N_1N_2(1+2N_3)}{(1-2N_3)(1-6N_3)} + \frac{2\Gamma Q\phi_E}{eN_o}\left(\frac{1}{1-6N_3}\right)\left(N + N_2^2 + \frac{4N_1^2}{1-2N_3}\right) \tag{5.20}$$

Note that N_3 is necessarily negative, so there are no singularities in (5.17-20). These equations are written in the order in which they will be solved, and are manifestly integrable. First, (5.17) is solved for N_3 after introducing the scaled time τ:

$$\tau = \frac{\Gamma Q}{eN_o}\int_0^t dt'\,\phi_E(t') , \tag{5.21}$$

where it will be recalled that $\phi_E(t)$ has the meaning of the physical driving potential in (5.3) evaluated at $x = \Lambda_o$, i.e.,

$$\phi_E(t) = \Lambda_o^2\,\tilde{\phi}_E(t) . \tag{5.22}$$

The solution of (5.17) is given in the implicit form

$$\frac{1}{6}\,\ell n\left[\frac{N_3}{N_3(0)}\right] - N_3 + N_3(0) = \tau \tag{5.23}$$

with $N_3(0) < 0$.

Combining (5.17) and (5.18) yields

$$\frac{\dot{N}_2}{N_2} = \frac{1}{3}\frac{\dot{N}_3}{N_3}\ ; \quad N_2 = N_2(0)\left[\frac{N_3}{N_3(0)}\right]^{1/3} . \tag{5.24}$$

Given N_2 and N_3, (5.19) for N_1 can be integrated in principle; in practice, this must be done numerically. Finally, with all the N_i known, (5.20) is integrated for N.

These last two equations contain the squared ratio

$$\xi \equiv \Lambda_D{}^2/\Lambda_o{}^2 \tag{5.25}$$

of the cross-over length Λ_D introduced in (4.10) and the inverted-V scale V_o. This is also the ratio of the ionization rate $T_I{}^{-1}$ (see (1.1)) to the nominal transport rate $T_D{}^{-1}$ (see (1.2)). We will treat ξ as a fixed parameter, although in principle it depends on the auroral potential drop $\phi-\phi_E$. This comes about because Λ_o (see (2.7)) depends on the Pedersen conductivity, which depends on the collision frequency, which depends on the average auroral deposition altitude in the ionosphere, which depends on the auroral energy. Since the auroral energy is in part controlled by ξ, there is an interesting feedback loop which we can only explore by going beyond the simplification of height-integration. The nominal value of ξ is somewhat less than one, but we expect that ξ will evolve to a value close to one as transport processes begin to be important on spatial scales comparable to Λ_D.

Before turning to the numerical solution of (5.19,20) we note that the four differential equations can be exactly integrated in the limit $|N_3| \ll 1$, in which case the solutions show a linear instability of the long-wave type discussed in Section 4:

$$N_3 = N_3(0)\ e^{6\tau} \tag{5.26}$$

$$N_2 = N_2(0)\ e^{2\tau} \tag{5.27}$$

$$N_1 = N_1(0)\ e^{4\tau} + \xi N_2(0)\ (e^{2\tau}-e^{4\tau}) \tag{5.28}$$

$$N = N(0)\ e^{2\tau} + N_2^{\ 2}(0)(1+3\xi^2)(e^{4\tau}-1)$$

$$+ \frac{7}{2}\xi N_2(0)[N_1(0)-\xi N_2(0)](e^{6\tau}-1) + \frac{4}{3}[N_1(0) - \xi N_2(0)]^2\ (e^{8\tau}-1)\ . \quad (5.29)$$

These solutions hold for arbitrary N_1 and N_2, but require $N_3 \ll 1$, and thus $N_3(0) \ll 1$, $\tau \lesssim 1/6$. Clearly, this small-N_3 case is an instability driven by the auroral ionization source.

Much more interesting is the large $|N_3|$ case, with $N_3 \ll -1$. This case is relevant when the auroral ionization source has produced a central ionospheric density which is large compared to the unperturbed density outside the aurora, and there are thus large gradients of density; they build up the transport terms, and allow the aurorally produced ionization to be carried away. We study this case by ignoring constants in terms like $1-6N_3 \to -6N_3$, etc., and find for N_i the power-law solutions:

$$N_3 = -\tau + O(\ell n\ \tau) \quad (5.30)$$

$$N_2 = A\tau^{1/3} + O(\tau^{-2/3}) \quad (5.31)$$

$$N_1 = -\frac{\xi A}{2}\tau^{4/3} + O(\tau^{1/3})\ , \quad (5.32)$$

where A is a constant of integration, and τ now stands for the scaled time of (5.21) plus the large positive constant $|N_3(0)|$.

As for N, substituting the above results in (5.20) yields a cancellation of the leading powers (which, if they had not cancelled, would have yielded $N \sim \tau^{5/3}$). This cancellation is a result of balance between ionization growth and transport loss, which comes about as the spatially dependent terms in the density, namely the N_i times powers of x or y, grow.

Further analytic progress seems to be impossible, so we turn to numerical calculations. We give results for the following case:

$$N(0) = 1,\ N_1(0) = 0,\ N_2(0) = 1,\ N_3(0) = -1,\ \xi = 1/2\ . \quad (5.33)$$

This corresponds to an auroral region where the initial potentials and density are symmetric around x = 0 (recall that x is a latitudinal distance variable), but have an E-W gradient as indicated by $N_2(0)$ and $\phi_2(0)$ (= 2/7, for our

parameters). We plot the initial density and potentials at $y = t = 0$ in Fig. 2. Here distances are measured in units of Λ_o, density scales with N_o, the density at $x = 0$, and the unit of potential is the auroral driving potential ϕ_E evaluated at a distance Λ_o from the origin. The return-current region (where $\phi-\phi_E \leq 0$) sets in at $|x| = x_c = .882$, at which point N returns its unperturbed value of .22. The plots in Fig. 2 qualitatively resemble both real auroral profiles and the exact stationary solutions of Cornwall [1988], as shown in Fig. 1. (Figs. 1 and 2 cannot be qualitatively compared, because of differences in normalizations, vertical and horizontal scales, and in actual physics.)

Fig. 3 shows the potentials and density at $y = 0$ and scaled time $\tau = 2$ (τ is defined in (5.21)). One sees that N has increased by about a factor of two, and its peak has shifted to the left, while the ionospheric potential ϕ is both decreased and flattened, while its minimum has moved to the right, opposite to the density shift. For other values of y at $\tau = 2$, add 1.41y to N and 0.16y to ϕ. There is, of course, no explicit indication of the generation of shorter length scales in Fig. 3, because the spatial dependence remains quadratic at all times. But an indication of the global breakdown of the quadratic ansatz can be seen in the minor inconsistencies between the position of the return current as determined by $\phi = \phi_E$ and by return of N to the undisturbed value of 0.22. One expects, as the perturbative analysis of Section 4 suggests, that generalizing the quadratic ansatz to repair the return-current inconsistencies will involve the unstable generation of shorter length scales. However, a linearized analysis at $\tau = 2$ is clearly inappropriate; the linearized solutions in (5.26-29) at $\tau = 2$ are far too large to be consistent with linear perturbation theory. What we would expect to see in a full-scale numerical analysis is that major features of the aurora (density maxima, potential minima) wander around through a finite fraction of Λ_o in times of order T_I or T_D, or some tens of seconds, while at the same time short-wavelength features begin to grow. All this happens even if the driving potential ϕ_E remains constant in time, as in our example. Naturally, in the real world ϕ_E also changes noticeably on these time scales, which further complicates the issue. Our point here is that such variations in ϕ_E are not necessary to produce auroral dynamics resembling what we in fact see, and that one cannot infer much about the dynamics of ϕ_E from the behavior of the auroral ionosphere on time scales of tens of seconds.

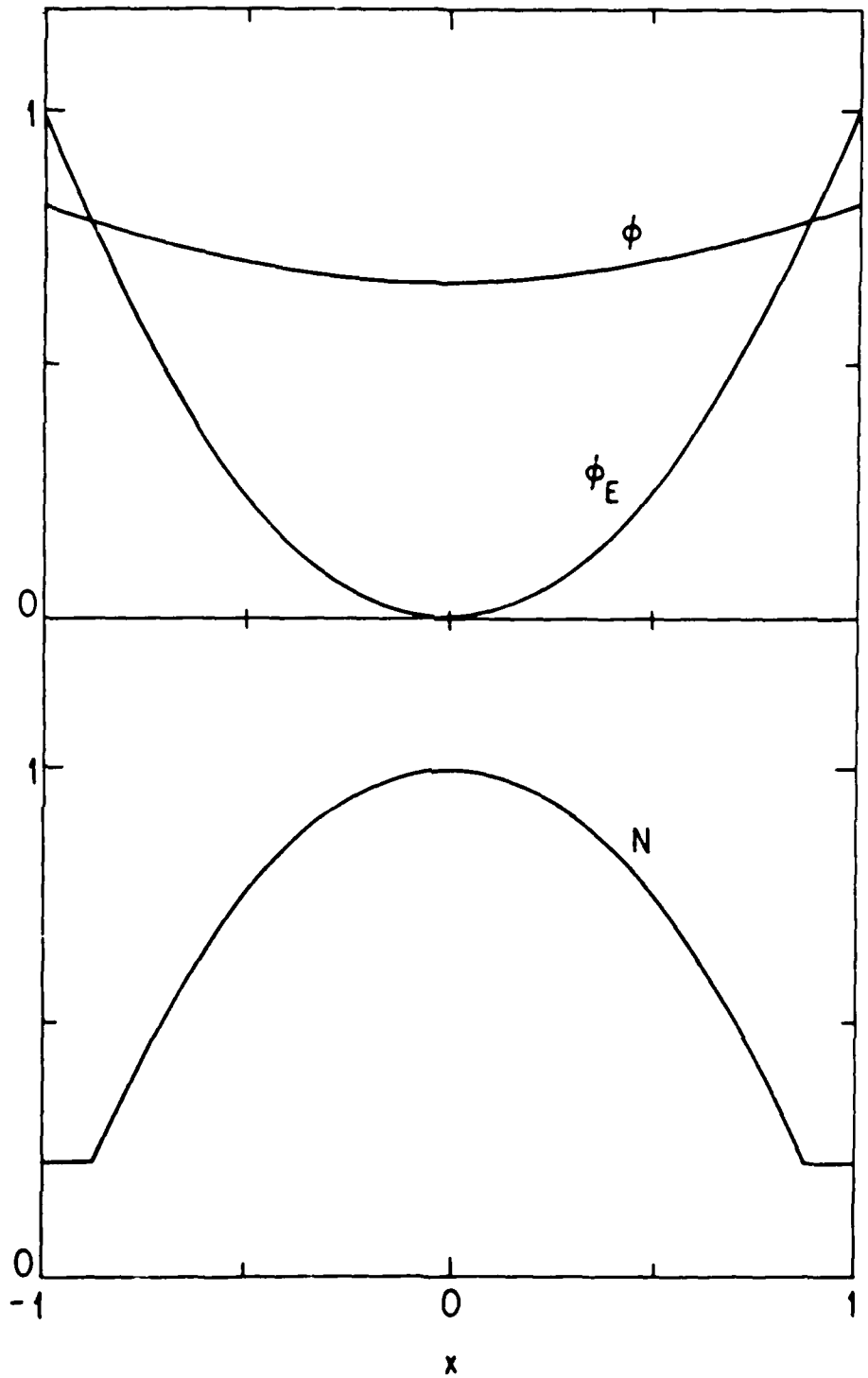

Fig 2. Potentials and Density at $\tau = 0$, $y = 0$ for a Time-Dependent Solution with no Recombination (ϕ_E Normalized to Unity at $|x| = 1$). The return-current region is at $|x| = 0.88$, where N has the ambient value 0.22 (in units of the density at $x = 0$). The distance scale is in units of Λ_o.

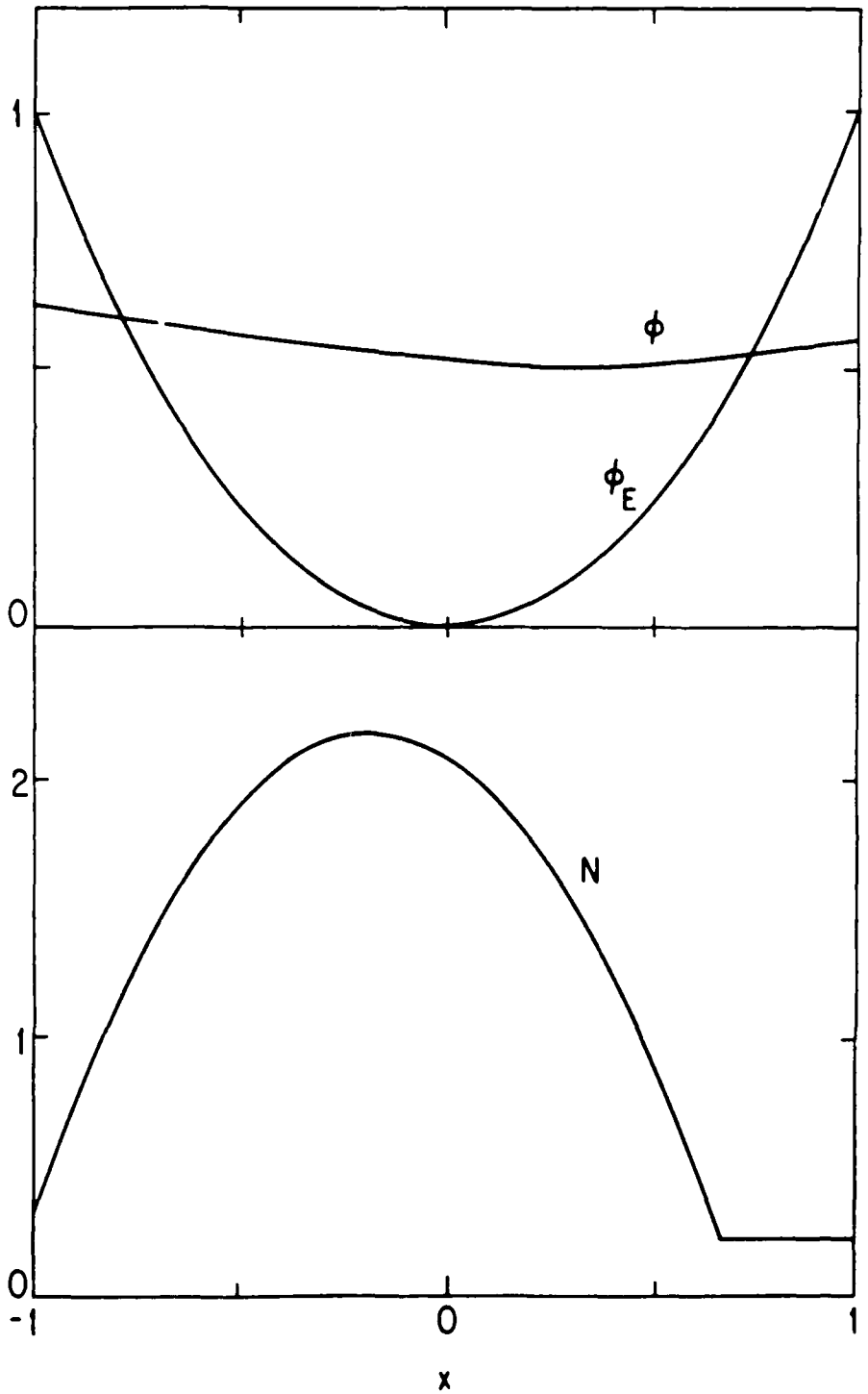

Fig 3. Potentials and Density at $\tau = 2$, $y = 0$ for a Time-Dependent Solution with no Recombination (ϕ_E Normalized to Unity at $|x| = 1$). The return-current region is at $|x| = 0.88$, where N has the ambient value 0.22 (in units of the density at $x = 0$). The distance scale is in units of Λ_0. The density maximum is shifted to the left and increased, while the potential is decreased and flattened, with its minimum moving to the right.

6. DISCUSSION

In this report we have investigated a new class of auroral-ionosphere instabilities driven by ionization from auroral electrons, and involving a parallel current which is linear in the ionosphere-magnetosphere potential drop. We emphasize that it is not the parallel current *per se* which drives the instability, but rather the ionization that it produces. The instability grows on a time scale of some tens of seconds (we assume that this is somewhat shorter than the nominal recombination time scale, which is true when auroral-ionosphere densities are not too large). This is comparable to transport time scales, but we have shown that there are necessarily regions in an aurora where transport alone cannot relieve the buildup of ionization, at least on the original (inverted-V) spatial scales of the aurora. Ultimately, dissociative recombination, proportional to the square of the density, will stabilize the produced ionization, but until then the aurora responds dynamically by lowering the magnetosphere-ionosphere potential drop; by generating small-scale fluctuations which are effective in transport; or by moving the region of low transport toward a region of lower density.

A linear local instability analysis of this problem is heuristically useful, but very limited practically because of the presence of zeroth-order density gradients. We supplant the linear analysis with a nonlinear analysis based on the hypothesis of quadratic spatial variations of potentials and density. This results in the replacement of the original pair of coupled nonlinear partial differential equations by four coupled, nonlinear ordinary differential equations. It is remarkable and unexpected that these equations are completely integrable. (A slight modification of the spatial variation leads to four coupled ordinary differential equations which are not obviously integrable; these may have chaotic solutions.) The solutions to the integrable equations reveal the expected transport phenomena discussed above.

In this report we have only discussed the case of a time-stationary driving magnetospheric potential, which leads to unstable auroral fluctuations on time scales of tens of seconds. The next step is to consider the case of time-dependent magnetospheric fluctuations, associated either with externally driven ULF waves in the appropriate frequency range (Pc 4-5; see Engbretson et al. [1986]) or as a magnetospheric feedback response to fluctuations in the auroral ionosphere.

REFERENCES

Basu, B., and B. Coppi, Velocity shear and fluctuations in the auroral regions of the ionosphere, J. Geophys. Res. 94, 5316, 1989.

Basu, Su., S. Basu, E. MacKenzie, P. F. Fougere, W. R. Coley, N. C. Maynard, J. D. Winningham, M. Sugiura, W. G. Hanson, and W. R. Hoegy, Simultaneous density and electric field fluctuation spectra associated with velocity shears in the auroral regions of the ionosphere, J. Geophys. Res. 93, 115, 1988.

Blomberg, L. G., and G. T. Marklund, The influence of conductivities consistent with field-aligned currents on high-latitude convection patterns, J. Geophys. Res. 93, 14,493, 1988.

Chiu, Y. T., and J. M. Cornwall, Electrostatic model of a quiet auroral arc, J. Geophys. Res. 85, 543, 1980.

Chiu, Y. T., A. L. Newman, and J. M. Cornwall, On the structures and mappings of auroral electrostatic potentials, J. Geophys. Res. 86, 10,029, 1981.

Chiu, Y. T., and M. Schulz, Self-consistent particle and parallel electric field distributions in the magnetospheric-ionospheric auroral region, J. Geophys. Res. 83, 629, 1978.

Cornwall, J. M., Exact solutions and low-frequency instability of the adiabatic auroral arc model, J. Geophys. Res. 93, 11,429, 1988.

Engbretson, M. J., L. J. Zanetti, T. A. Potemra, and M. H. Acuña, Harmonically structural ULF pulsations observed by the AMPTE CCE magnetic field experiment, Geophys. Res. Letters 13, 905, 1986.

Fejer, B. G., Ionospheric plasma turbulence in the high latitude E region, in Physics of Space Plasmas (1988), edited by T. Chang et al., p. 15, Scientific Publishers, Cambridge, 1989.

Ganguli, G., Y. C. Lee, and P. J. Palmadesso, Electrostatic ion cyclotron instability due to a nonuniform electric field perpendicular to the external magnetic field, Phys. Fluids 28, 761, 1985.

Gorney, D. J., A study of the spatial scales of discrete auroral arcs, in Physics of Space Plasmas (1988), edited by T. Chang et al., p. 385, Scientific Publishers, Cambridge, 1989.

Hallinan, J. J., and T. N. Davis, Small scale auroral arc distortions, Planet. Space Sci. 18, 1735, 1970.

Huba, J. D., Theoretical and simulation methods applied to high latitude ionospheric turbulence, in Physics of Space Plasmas (1988), edited by T. Chang et al., Scientific Publishers, Cambridge, 1989.

Keskinen, M. J., and S. L. Ossakow, Theories of high latitude ionospheric irregularities: A review, Radio Sci. 18, 1077, 1983.

Keskinen, M. J., H. G. Mitchell, J. A. Fedder, P. Satyanarayana, S. T. Zalesak, and J. D. Huba, Nonlinear evolution of the Kelvin-Helmholtz instability in the high-latitude ionosphere, J. Geophys. Res. 93, 137, 1988.

Kintner, P. M., and C. E. Seyler, The status of observations and theory of high latitude ionospheric and magnetospheric plasma turbulence, Space Sci. Rev. 40, 1123, 1985.

Labelle, J., R. Sica, C. Kletzing, G. Earle, M. Kelley, D. Lummerzheim, R. Torbert, K. Baker, and G. Berg, Ionization from soft electron precipitation in the auroral F region, J. Geophys. Res. 94, 3791, 1989.

Linson, L., and J. Workman, Formation of striations in ionospheric plasma clouds, J. Geophys. Res. 75, 3211, 1970.

Lotko, W., B. U. Ö. Sonnerup, and R. L. Lysak, Nonsteady boundary layer flow including ionospheric drag and parallel electric fields, J. Geophys. Res. 92, 8635, 1987.

Lyons, L. R., Generation of large-scale regions of auroral currents, electric potentials by the divergence of the convection electric field, J. Geophys. Res. 85, 17, 1980.

Lyons, L. R., Discrete aurora as the direct result of an infrared high-altitude generating potential distribution, J. Geophys. Res. 86, 1, 1981.

Mitchell, H. G., J. A. Fedder, M. J. Keskinen, and S. T. Zalesak, A simulation of high latitude F-layer instabilities in the presence of magnetosphere-ionospheric coupling, Geophys. Res. Letters 12, 283, 1985.

Reiff, P., H. Collin, J. Craven, J. Burch, J. Winningham, E. Shelley, L. Frank, and M. Friedman, Determination of auroral electrostatic potentials using high- and low-altitude particle distributions, J. Geophys. Res. 93, 7441, 1988.

Weimer, D. R., C. K. Goertz, D. A. Gurnett, N. C. Maynard, and J. L. Burch, Auroral zone electric fields from DE1 and 2 at magnetic conjunctions, J. Geophys. Res. 90, 7479, 1985.

Weimer, D. R., D. A. Gurnett, C. K. Goertz, J. D. Meniotti, J. L. Burch, and M. Sugiura, The current-voltage relation in auroral current sheets, J. Geophys. Res. 92, 187, 1987.

Weimer, D. R., N. C. Maynard, W. J. Burke, and M. Sugiura, Stationary auroral current oscillations resulting from the magnetospheric generator, J. Geophys. Res. 93, 11,436, 1988.

APPENDIX

Here we very briefly describe a generalization of the integrable model of Section 5, which uses a more general quadratic ansatz for ϕ, N, and ϕ_E rather than the specialized forms (5.1,2,3). The only point to be made is that the resulting four nonlinear differential equations in time are not obviously integrable, and so their solution may be chaotic.

The ansatz we use is

$$\phi = \tilde{\phi}(t) + x_i A_{ij} x_j \tag{A.1}$$

$$N = \tilde{N}(t) + x_i D_{ij} x_j \tag{A.2}$$

$$\phi_E = x_i \tilde{\phi}_{Eij} x_j \ . \tag{A.3}$$

where A, D, and $\tilde{\phi}_E$ are symmetric 2 × 2 matrices depending on t, and the two-dimensional vector x_i has components $x_1 = x$, $x_2 = y$; repeated indices are summed over. Note that this is not the *most general* quadratic ansatz, since terms linear in x_i could be added to the RHS of (A.1,2,3). We need not deal with this additional complication, which only reinforces the lack of obvious integrability.

As in Section 5, we drop the tildes on the RHS of (A.1,2,3) and we scale lengths with Λ_o and densities with N_o (see 5.8)). Then in the formulas below N and the matrix D are dimensionless, while A and ϕ_E have the dimensions of potential. Inserting the ansatz into the basic equations (2.4,5) with $\alpha = 0$ yields:

$$\mathrm{Tr}\ A = \phi/2N \tag{A.4}$$

$$D\ \mathrm{Tr}\ A + \{A,D\} = \frac{1}{2}\ (A-\phi_E) \tag{A.5}$$

$$\dot{N} = \frac{\Gamma Q}{eN_o}\ \phi \tag{A.6}$$

$$\dot{D} + \frac{2c}{B\Lambda_o^{\ 2}}\ (A\varepsilon D - D\varepsilon A) = \frac{\Gamma Q}{N_o e}\ (A-\phi_E)\ . \tag{A.7}$$

In these equations,

LABORATORY OPERATIONS

The Aerospace Corporation functions as an "architect-engineer" for national security projects, specializing in advanced military space systems. Providing research support, the corporation's Laboratory Operations conducts experimental and theoretical investigations that focus on the application of scientific and technical advances to such systems. Vital to the success of these investigations is the technical staff's wide-ranging expertise and its ability to stay current with new developments. This expertise is enhanced by a research program aimed at dealing with the many problems associated with rapidly evolving space systems. Contributing their capabilities to the research effort are these individual laboratories:

Aerophysics Laboratory: Launch vehicle and reentry fluid mechanics, heat transfer and flight dynamics; chemical and electric propulsion, propellant chemistry, chemical dynamics, environmental chemistry, trace detection; spacecraft structural mechanics, contamination, thermal and structural control; high temperature thermomechanics, gas kinetics and radiation; cw and pulsed chemical and excimer laser development, including chemical kinetics, spectroscopy, optical resonators, beam control, atmospheric propagation, laser effects and countermeasures.

Chemistry and Physics Laboratory: Atmospheric chemical reactions, atmospheric optics, light scattering, state-specific chemical reactions and radiative signatures of missile plumes, sensor out-of-field-of-view rejection, applied laser spectroscopy, laser chemistry, laser optoelectronics, solar cell physics, battery electrochemistry, space vacuum and radiation effects on materials, lubrication and surface phenomena, thermionic emission, photosensitive materials and detectors, atomic frequency standards, and environmental chemistry.

Electronics Research Laboratory: Microelectronics, solid-state device physics, compound semiconductors, radiation hardening; electro-optics, quantum electronics, solid-state lasers, optical propagation and communications; microwave semiconductor devices, microwave/millimeter wave measurements, diagnostics and radiometry, microwave/millimeter wave thermionic devices; atomic time and frequency standards; antennas, rf systems, electromagnetic propagation phenomena, space communication systems.

Materials Sciences Laboratory: Development of new materials: metals, alloys, ceramics, polymers and their composites, and new forms of carbon; nondestructive evaluation, component failure analysis and reliability; fracture mechanics and stress corrosion; analysis and evaluation of materials at cryogenic and elevated temperatures as well as in space and enemy-induced environments.

Space Sciences Laboratory: Magnetospheric, auroral and cosmic ray physics, wave-particle interactions, magnetospheric plasma waves; atmospheric and ionospheric physics, density and composition of the upper atmosphere, remote sensing using atmospheric radiation; solar physics, infrared astronomy, infrared signature analysis; effects of solar activity, magnetic storms and nuclear explosions on the earth's atmosphere, ionosphere and magnetosphere; effects of electromagnetic and particulate radiations on space systems; space instrumentation.